



HAL
open science

Anatomy Transfer

Ali Hamadi Dicko, Tiantian Liu, Benjamin Gilles, Ladislav Kavan, François Faure, Olivier Palombi, Marie-Paule Cani

► **To cite this version:**

Ali Hamadi Dicko, Tiantian Liu, Benjamin Gilles, Ladislav Kavan, François Faure, et al.. Anatomy Transfer. ACM Transactions on Graphics, 2013, ACM SIGGRAPH ASIA, 32 (6), pp.Article No. 188. 10.1145/2508363.2508415 . hal-00862502

HAL Id: hal-00862502

<https://inria.hal.science/hal-00862502>

Submitted on 16 Sep 2013

HAL is a multi-disciplinary open access archive for the deposit and dissemination of scientific research documents, whether they are published or not. The documents may come from teaching and research institutions in France or abroad, or from public or private research centers.

L'archive ouverte pluridisciplinaire **HAL**, est destinée au dépôt et à la diffusion de documents scientifiques de niveau recherche, publiés ou non, émanant des établissements d'enseignement et de recherche français ou étrangers, des laboratoires publics ou privés.

Anatomy Transfer

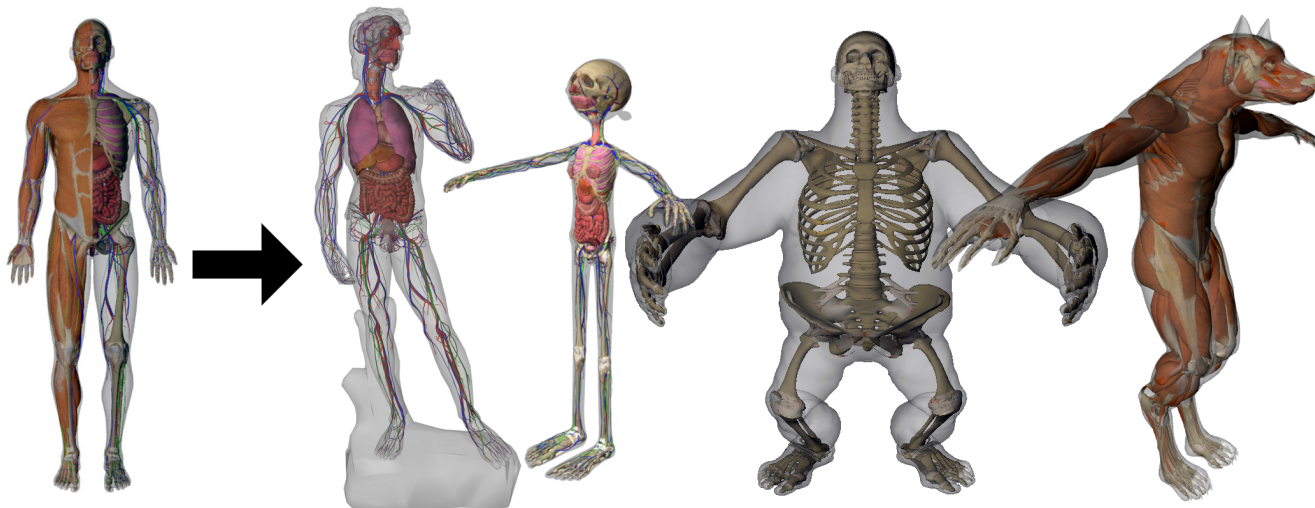


Figure 1: A reference anatomy (left) is automatically transferred to arbitrary humanoid characters. This is achieved by combining interpolated skin correspondences with anatomical rules.

Abstract

Characters with precise internal anatomy are important in film and visual effects, as well as in medical applications. We propose the first semi-automatic method for creating anatomical structures, such as bones, muscles, viscera and fat tissues. This is done by transferring a reference anatomical model from an input template to an arbitrary target character, only defined by its boundary representation (skin). The fat distribution of the target character needs to be specified. We can either infer this information from MRI data, or allow the users to express their creative intent through a new editing tool. The rest of our method runs automatically: it first transfers the bones to the target character, while maintaining their structure as much as possible. The bone layer, along with the target skin eroded using the fat thickness information, are then used to define a volume where we map the internal anatomy of the source model using harmonic (Laplacian) deformation. This way, we are able to quickly generate anatomical models for a large range of target characters, while maintaining anatomical constraints.

CR Categories: I.3.7 [Computer Graphics]: Three-Dimensional Graphics and Realism—Animation

Keywords: Character modeling

1 Introduction

A high level of anatomical precision is necessary in many Computer Graphics applications, from visualizing the internal anatomy for education purposes, to anatomical simulation for feature films, ergonomics, medical, or biomechanical applications (e.g. optimizing muscle energy). Highly realistic animations showing muscles or tendons deforming the skin typically require precise anatomical models. Moreover, the control of the fat distribution is important for achieving the associated secondary dynamics effects. While a lot of research addresses the challenge of fast and accurate simulation, we focus on the upstream part of the pipeline, modeling anatomy.

The current tools available for artists to model anatomical deformations [Maya-Muscle 2013] as well as early academic work [Wil-

helms and Van Gelder 1997; Scheepers et al. 1997] extensively rely on user input, essentially amounting to setting up the musculature from scratch. Recent years witnessed huge improvements in anatomically-based simulation, especially in terms of computational efficiency [Patterson et al. 2012]. However, the cost of setting up a 3D anatomical model for a given character remains. This task is very time consuming and tedious, as it requires modeling of the bones, organs, muscles, and connective and fat tissues. With real humans, it is possible to take advantage of 3D imaging, such as MRI [Blemker et al. 2007]. However, this route is difficult or even impossible for fictional characters, ranging from Popeye to Avatar’s Na’vi.

A naive idea to solve the problem would be to transfer the anatomy from a reference character to the target in a purely geometric way. It is obvious this route has a number of shortcomings: humanoids are made of bones, viscera, muscles, and fat tissues. Specific anatomical rules need to be preserved in order to generate a plausible anatomical structure: bones should remain straight and symmetric, and the distribution of fat, which may vary from one individual to another, should be taken into account while transferring muscles and viscera. CG characters can also contain non-anatomical or stylized components, such as hair, a shell, or even clothes. A specific problem is to prevent the internal anatomical structure to fill these areas, as we want our method to work even in these challenging cases.

We propose a semi-automatic method for creating the internal anatomy of any target character by transferring the internal anatomy of a highly-detailed anatomical model with minimal fat layers (Zygote body). Our method starts by registering the skins (outer boundaries) of the two models. An initial deformation between the two volumes is established using Laplacian deformation. The Laplacian is however uninformed about the anatomy and can, e.g., bend or otherwise unnaturally deform the bones. Therefore, we impose a number of anatomical constraints, such as requiring the bones to remain quasi-rigid. We also provide a tool for carving out the fat layers as well as the non-anatomical parts of the volume of the target model, before transferring the muscles and viscera. Our specific contributions are:

- a novel registration method to transfer a source anatomy to

characters with very different shapes while exploiting anatomical knowledge to get a plausible result;

- the use of a texture, specifying non-uniform distribution of fat under the skin of a character, and a robust method to erode the internal volume accordingly;
- a user-friendly tool for editing the fat distribution texture, if needed, on a per bone basis.

We exploit prior knowledge about human anatomy, e.g., we require that bone shapes and sizes remain as close as possible to human, by restricting the deformation modes and enforcing symmetry during registration.

The journey towards realistic Computer Graphics humans starts with modeling. To our knowledge, this work is the first attempt to address the challenging goal of semi-automatic anatomy authoring. While many limitations and open questions remain, we hope that our method opens the door to inexpensive anatomy authoring tools and helps to promote and democratize applications leveraging anatomically-based simulation and visualization.

2 Related work

Skeleton-based models have been used in computer graphics to control the motion of the human body or its interaction with objects using joint torques, see e.g. [Faloutsos et al. 2001; Zordan et al. 2005] for full body, and [Pollard and Zordan 2005; Kry and Pai 2006] for the hand. [Baran and Popović 2007] presented a method for automatic rigging of character skins without internal anatomy, except for automatically inferred animation skeleton. Musculoskeletal models have been proposed to animate muscle deformations [Wilhelms and Van Gelder 1997; Scheepers et al. 1997; Aubel and Thalmann 2001], to perform facial animation [Waters 1987; Sifakis et al. 2005], to study or improve the control [Lee and Terzopoulos 2006; Wei et al. 2010; Wang et al. 2012], or to increase the quality of the flesh and skin deformations [Lee et al. 2009]. Beyond bones and muscles, [Sueda et al. 2008] demonstrated an impressive model including detailed bones, joints, skin, and tendons. The deformations of the skin due to the tendon actuators dramatically improve the resulting quality. The windpipe is visible in an increasing number of feature animation characters, and the veins increase the realism of the skin.

While encouraging results have been demonstrated for transferring deformations from one model to another [Sumner and Popović 2004], little has been done in terms of volumetric geometry transfer across shapes. A lot of effort has been dedicated to solving the registration problem: the computation of correspondences between objects, mainly between surface meshes or images. Registration is a fundamental problem in computer science, especially in computer graphics [Kaick et al. 2011]. Most registration methods alternate between two steps: A) the estimation of sparse correspondences, optimizing the extrinsic (e.g., closest points [Besl and McKay 1992]) or intrinsic (e.g., [Bronstein et al. 2008]) similarity; and B) correspondence completion and regularization to achieve plausible dense displacement fields. To improve the robustness of the registration with respect to object poses (i.e., rigid transforms, isometry, etc.), different isometry invariant parameterizations have been proposed such as spectral embedding [Mateus et al. 2008], conformal mapping [Lipman and Funkhouser 2009], or functional maps [Ovsjanikov et al. 2012]. On the other hand, robustness to topological noise and to partial data can be achieved from extrinsic correspondences (i.e. established in Cartesian space) [Li et al. 2008; Huang et al. 2008]. For regularization, a displacement model is often associated: ranging from rigid, affine, to as-rigid-as-possible deformation fields, possibly with extra constraints

such as articulations [Gilles et al. 2010]. Our method can be seen as a partial registration process, where skin surfaces are first registered based on the data, and the interior estimated using interpolation and anatomical rules.

3 Overview

The anatomy of a living body depends on numerous physiological constraints. The huge variability of anatomy is constrained by critical anatomical rules. We propose semi-automatic modeling of humanoid anatomy that uses these rules to constrain the resulting volumetric deformation, aiming to achieve as-anatomical-as-possible results. For the skeleton, our pipeline relies on the rule that bones must stay straight at the end of the anatomy transfer (R1), and symmetric across the sagittal plane (R2). The third rule is the fact that there is no relation between the quantity of fat tissue and the size of the bones [Moore and Dalley 1999]. For example, a fat character has the same skeleton as a lean one (R3), but the muscularity is proportional to keep up the body (R4) [M. Gilroy 2008]. The fat tissues are localized mainly between the skin and the muscles (R5) [M. Gilroy 2008]. They can be interpreted as a stock of energy and therefore, the amount of fat tissue can be very variable. During anatomy transfer, anatomical structures cannot disappear (R6), and the muscular insertion points are preserved (R7).

Our anatomy transfer pipeline implementing these rules is illustrated using a didactic anatomy piece in Fig. 2. The user provides the skin of a target character and may add a user-defined distribution of sub-skin fat (possibly including other non-anatomical structures) modeled using a thickness function in texture space (Fig. 2.a). As an alternative to user defined fat map, this information can be also extracted from real MRI data. Our method requires that the source (reference character) and target skin share the same (u, v) texture space. The first step, not shown in the figure, is thus to compute the registration of the source and the target skin (Sec.4).

Our source model (Fig. 2.c) is composed of bones, skin, muscles and viscera, and it includes almost no fat. We therefore erode the volume of the target (Fig. 2.b) according to the thickness of the fat layer, to warp our “lean” source anatomy to the sub-fat part of the target volume (Sec. 5), following rule (R5). The user can create the thickness data for stylized and cartoony characters using our new semi-automatic tool (Sec. 6).

The displacement of the skin from the source to the eroded target is then interpolated within the volume to transfer the internal anatomy (Sec. 7). This, along with a reasonable choice of fat thickness, enables us to follow rules (R3) and (R4). However, naively interpolating the skin deformation generally results in visible artifacts in the internal anatomy, especially in the skeleton, which may exhibit bent or inflated bones. We thus use this interpolation (Fig. 2.d) as an attractor for a constrained registration (Fig. 2.f), where the constraints express anatomical properties, such as the symmetry of the skeleton about the sagittal plane (Sec. 8). This allows us to incorporate rules (R1) and (R2). This constrained registration provides us with a plausible skeleton which fits the shape of the target character while following the anatomical rules.

Finally, we compute a new interpolating deformation field, using the internal skeleton as well as the eroded shape as boundary conditions (Fig. 2.e). This allows us to interpolate the remaining anatomical entities in between. This preserves all the anatomical structures and their relative locations, and satisfies rules (R6) and (R7).

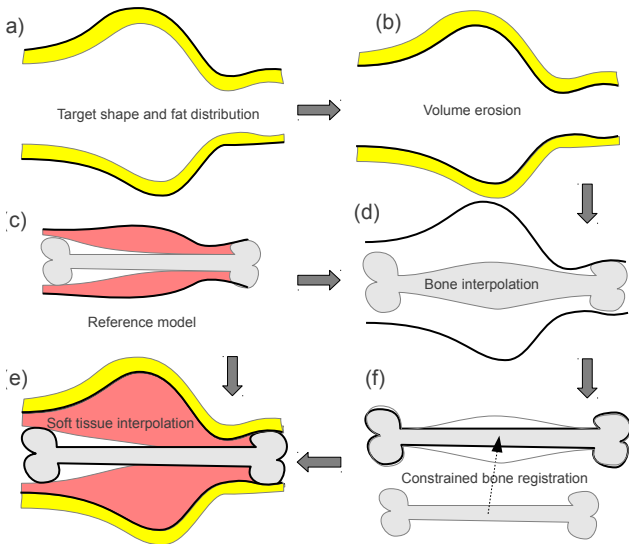


Figure 2: Anatomy transfer pipeline.

4 Skin registration

The first step of our pipeline is to establish surface correspondences between the source and target skins. Because skins of different subjects are not isometric, we focus on extrinsic correspondences for registration. For simplicity, we compute closest point correspondences such as in the popular Iterative Closest Point algorithm [Besl and McKay 1992]. Based on correspondences established at each iteration, a smooth as-rigid-as-possible deformation field for the source skin is updated. As in [Gillet et al. 2010], we use the shape matching deformation method [Müller et al. 2005] which is both efficient (being based only on geometry) and controllable. Skin stiffness is progressively decreased during the registration to reduce sensitivity to local minima. Manual initialization is performed in the case of large differences between the pose of the source and target characters.

5 Volume erosion

The internal volume of the target character is composed of the skeleton and the soft tissues modeled in the source anatomy, along with a significant volume of fat tissue, which is usually not explicitly represented in anatomical models, including ours¹, and therefore difficult to model. We thus consider only a sub-skin layer of the fat tissue, which separates the skin from the rest of the anatomy. This layer, which may have a significant thickness depending on the target character, reduces the available volume for the skeleton and muscles. The layer of fat below the skin is not uniform around the body. It is well-known that men and women exhibit different distributions, and this distribution may also vary between individuals [Gray and Lewis 1918]. With realistic human models, we make the simplifying assumption that each gender can be associated with one scalable distribution.

The simplest way to model the distribution of fat is to add a channel to the texture of the skin to represent the local thickness of the fat layer. We compute this thickness using the MRI image of a real person. We first tag the voxels corresponding to the skin and to the fat layer using a segmentation technique. Relying on the local normal to associate each voxel of the skin to a thickness would not

be reliable due to skin curvature and imperfections in the input data. We therefore rely on discrete data, exploiting voxel neighborhoods. We compute a forest of shortest paths from the skin voxels to the fat voxels, where each skin voxel is the root of a tree. Then for each skin voxel we set the local fat thickness to the maximum distance to the leaves of its tree. Based on the texture coordinates of the skin voxels and the associated thickness, we interpolate the value at each pixel of the thickness texture.

The thickness texture can be edited as discussed in Section 6, and then used to perform volume erosion (Fig. 2.b). For each vertex of the target, we compute the local depth using the texture coordinates and we move the vertex by this distance following the forest of shortest paths. An example result is shown in Fig. 5.

6 Edition of the fat distribution texture

In order to generate fat distribution textures for arbitrary characters, we created a “fat editor” that provides both physically plausible initialization and full artistic control. Based on the observation that fat distribution is close to uniform around each bone, we adopted the idea of bounded biharmonic weights [Jacobson et al. 2011] to create smooth fat distribution maps. We set the bones as boundary constraints and minimize biharmonic (Laplacian) energy subject to these constraints. This way, we smoothly spread influence from the bones to the skin and obtain a fat map by tuning only a few parameters. Choosing a reasonable thickness leaves space for a realistic amount of muscle tissue (rule R4).

Fig. 3 shows the pipeline of our fat editor. The editor first loads the target character model and its bones calculated using our bone registration. Similarly to [Kavan and Sorkine 2012], we compute bounded biharmonic weights using a regular voxel grid, obtained using the Binvox program [Binvox 2013]. After pre-computing the weights, users can very quickly tune the amount of fat distribution around each bone. For example, we can assign 0.4 to the pelvis and sacrum bones to model the fat around the character belly, but give 0 to the skull because there is no fat beneath his scalp. The editor computes linear combination of pre-computed bone weights with the control parameters set by the users to generate the final fat distribution map.

The fat editor does not have to use only the anatomical bones. If artists want to control the fat around a certain region with more details, they can add fictional bones inside that region and tune the new parameters introduced by the fictional bones. We did not do this in our examples because we were satisfied with the results using only anatomical bones.

7 Interpolation

In our framework, volumetric interpolation is required at two stages of the method: 1) to initialize bones inside the eroded skin, and 2) when soft organs are transferred, using both the eroded skin and the bones as boundary conditions. This section describes the interpolation method we use in both cases.

Given boundary conditions on the displacement field, we solve for the displacements in the interior by minimizing the harmonic energy, also known as Laplace interpolation [Press et al. 2002]. The principle is to compute as linear as possible interpolation by requiring zero value of the Laplacian of the displacement field at each unconstrained voxel. The boundary displacements \bar{f} are incorporated as hard constraints:

$$\begin{aligned} \nabla^2 f(x) &= 0, x \text{ inside} & (1) \\ f(x) &= \bar{f}, x \text{ on the boundary} & (2) \end{aligned}$$

¹www.zygot.com

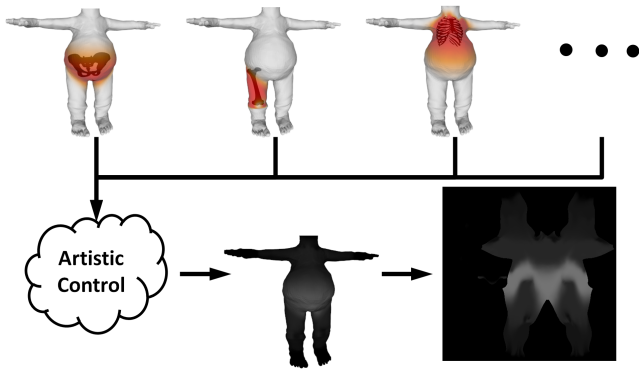


Figure 3: Fat distribution texture generation for the character. Top (initialization): we use bounded biharmonic weights to compute skin weights corresponding to each bone. Bottom (fat editing): artists can set fat parameters and generate fat distribution map. Brighter regions correspond to thicker fat layers.

284 The discretization on our grid results in a large sparse system of linear
 285 equations, which we solve using the Conjugate Gradient solver
 286 from the Eigen library [Guennebaud et al. 2010]. More sophisticated
 287 methods such as a multigrid solver with an efficient handling
 288 of irregular boundaries [Zhu et al. 2010] could be used to further
 289 accelerate the computation.

8 Bone registration

291 Bones directly deformed using the method presented in Section 7
 292 may become non-realistically stretched or bent, as illustrated in
 293 Fig. 2.d. The difference of shape between real or plausible charac-
 294 ters and the reference anatomy is due to a different size as well as a
 295 different amount of soft tissue around them. Changes of character
 296 size mainly scales up or down the bones, while the changes of soft
 297 tissue do not modify the bones. We thus restrict each bone trans-
 298 formation to an affine transformation, using the initial interpolated
 299 bone as an attractor to a plausible location inside the body. More-
 300 over, the symmetry of the trunk is enforced by deforming it using
 301 transformations centered in the sagittal plane. We did not impose
 302 symmetry constraints for pairs of corresponding bones to allow the
 303 input of non-symmetric target characters, such as the David model
 304 in our examples. The constrained minimization is performed by
 305 attaching all the voxels of the reference bone to a common affine
 306 frame and attracting them to their interpolated position using linear
 307 springs. We have not noticed any visible artifacts due to the possi-
 308 ble shearing modes introduced by the affine transformations. We
 309 use an implicit solver to ensure stability [Baraff and Witkin 1998].
 310 Organ intersections do not occur when the interpolation is foldover-
 311 free, which is the case in all our examples: during the semi-rigid
 312 bone registration, the offsets between the interpolated bones and the
 313 registered bones mostly occur in the off-axis directions, so we have
 314 not encountered any intersection. If necessary, this issue could be
 315 addressed using standard collision handling routines.

316 Fig. 4 illustrates the benefits of bone registration compared to sim-
 317 ple interpolation. Notice the bent bones in the legs, the oddly in-
 318 flated bones in the arms of the interpolated skeleton, as well as the
 319 broken symmetry of the rib cage are fixed by the affine registration.
 320 Moreover, the shape of the skull is influenced by the hair during the
 321 interpolation. This deformation is also filtered out by the affine
 322 transformation.

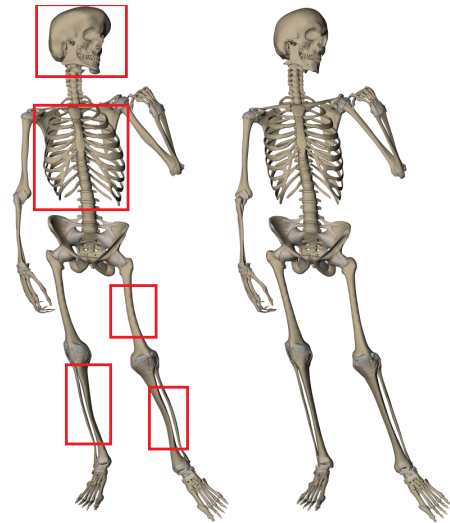


Figure 4: The benefits of bone registration. Left: after interpolation only. Right: after affine registration.

9 Results

324 We have successfully applied our framework to both realistic and
 325 cartoon characters, as can be seen in Fig. 1. Cartoon characters
 326 were not intended as a primary motivation for anatomically-based
 327 modeling, but they are a challenging stress test for the system,
 328 showing how far from the input model we can go.

329 A nice feature of our method is that what we actually compute a
 330 deformation field, which can be used to transfer arbitrarily com-
 331 plex internal geometry. Once this computation is achieved, we are
 332 able to transfer a complete anatomy including bones, muscles, lig-
 333 aments, viscera, blood vessels, nerves etc. very quickly. Our fat
 334 editor allows an artist to tailor a distribution for a specific target
 character, as shown in Fig. 5. Other examples of anatomy transfer

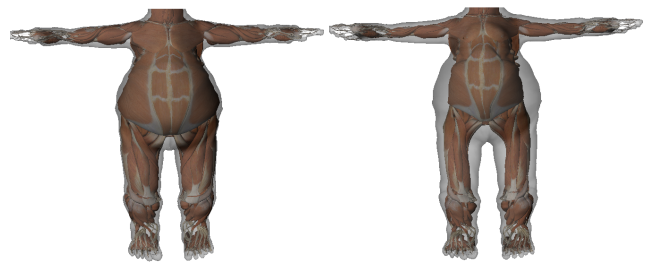


Figure 5: Transfer to a fat character. Left: without erosion. Right: a preliminary erosion accounts for the fat and results in a more plausible muscular system.

335 are shown in Fig. 6.

336
 337 The reconstruction of Popeye in Fig. 7 exhibits a surprising chin,
 338 which could be mitigated using fat. Note, however, that his fore-
 339 arm bones are realistic despite the odd external shape. Fig. 7 also
 340 shows the reconstruction of the anatomy of Olive, a very thin char-
 341 acter. We can notice how close her muscles are to her skin while
 342 her skeleton remains thin, but well adapted to her morphology.



Figure 6: Brutus blood vessels and nerves.



Figure 7: Popeye and Olive.

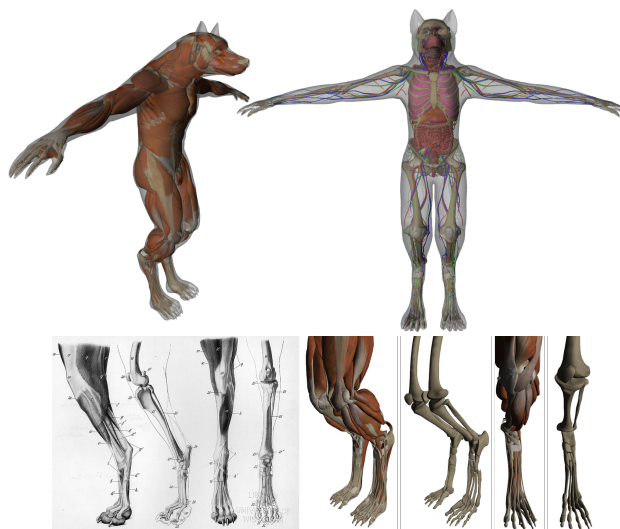


Figure 8: Top: Werewolf musculature, skeleton, and internal organs. Bottom: Comparison between werewolf lower limb and real wolf lower limb.

343 To see how far we can push the concept of anatomy transfer, we
 344 transferred our reference model into a werewolf (half human and
 345 half animal). Fig. 8 demonstrates how the human anatomy fits ac-
 346 curately within the body of this monster despite of the difference in
 347 morphology. The bottom of Fig. 8 validates the transfer by compar-
 348 ing the results we get with the musculoskeletal system of a real
 349 wolf (*Canis lupus*), shown on the left.

350 Fig. 9 shows the reconstruction of a real male based on his MRI
 351 image. The muscles are surprisingly well captured in the lower legs,
 352 the bottom cheeks and the trunk. Some muscles are not accurately
 353 reconstructed, due to different relative sizes in the real person and
 354 our reference model and to errors in skin registration. The latter are
 355 also responsible for inaccuracies in the fat layer. The goal of this
 356 reconstruction attempt is not to compete with established segmen-
 357 tation methods, but to suggest that anatomy transfer may provide
 358 a useful initial estimate. Moreover, a lot of thin anatomical struc-
 359 tures which cannot be seen in the volumetric image are present in
 360 our model. In future work, complementing our framework with
 361 sparser but more accurate segmentation methods may provide use-
 362 ful constraints to insert in our interpolation, to accurately infer the
 363 positions of the features invisible in the MRI.

364 Our methods provides significant improvements over a shape
 365 matching method like [Gilles et al. 2010], which is based on differ-
 366 ent premises. They assume noisy MRI input and therefore employ
 367 approximate volumetric shape matching, while our method assumes
 368 exact correspondence between the input and the target surfaces, i.e.,
 369 the deformation field has to interpolate rather than approximate the
 370 boundary. To make [Gilles et al. 2010] as interpolant as possible,
 371 we need to make the shape matching stiffness and cluster size small
 372 enough, thereby slowing down the convergence and requiring a suffi-
 373 ciently dense mesh. A comparison is shown in

374 Fig. 10. In the result of [Gilles et al. 2010] the internal tissue inter-
 375 sects the skin (lower arm, chest) and the matching is less accurate,
 376 as can be seen near the biceps, the shoulder, and the neck. More-
 377 over, symmetry is visibly violated in the lower abdominal muscles
 378 and between the arms. Finally, the computation time was 30 min-
 379 utes for [Gilles et al. 2010] due to the small size of the clusters,
 380 while our Laplacian solution converged in only 3 minutes.

381 In Fig. 11, 12, 13, we present some example of useful anatomy
 382 transfers. In Fig. 11 we show a transfer of an articulated system,
 383 animation and skinning [Kavan et al. 2008]. The joint orientations
 384 match the character posture, and the resulting motion is similar for
 385 all characters, as can be seen in the accompanying video. Fig. 12
 386 shows a transfer of muscle lines of action [Thelen 2003] for phys-
 387 ical simulations. Using the same muscle activations, we are able
 388 to create similar movements, such as knee flexion or hip rotation,
 389 for both the reference model and the target (see the accompany-
 390 ing video). These action lines attached to the bones at both ends
 391 could be transferred directly. However, more realistic muscle paths
 392 include via points along muscle center lines or around warp sur-
 393 faces on bone geometry, and this requires full volumetric transfer,
 394 because these points cannot be entirely defined with respect to skin
 395 and bone surfaces. In Fig. 13 we present a transfer of deformation,
 396 mimicking bicep bulging in David's arm.

397 We use a standard laptop computer with an Intel CoreI7 processor at
 398 3 GHz and 8GB of RAM. For each character, the total computation
 399 time ranges from a couple of seconds to less than five minutes with
 400 our current implementation. Fat erosion takes about one minute in
 401 a $64 \times 171 \times 31$ volumetric image, and the first Laplacian interpo-
 402 lation takes 15s in the same grid. The bone registration takes about
 403 3 minutes. Most of the computation time is spent in the final Lapla-
 404 cian interpolation, which requires a finer resolution to get a smooth
 405 result. In a $309 \times 839 \times 142$ grid, it takes less than 5 minutes. Once
 406 the displacement field is computed, transferring the 500MB of geo-
 407 metry of our model takes less than a minute. In future work, we
 408 plan to replace our interpolation solver with a highly parallel GPU
 409 interpolation.

410 Our method has a number of limitations. Firstly, automatically infer-
 411 ring non-standard distributions of fat from the morphology of the
 412 character would be an interesting extension. Standard human

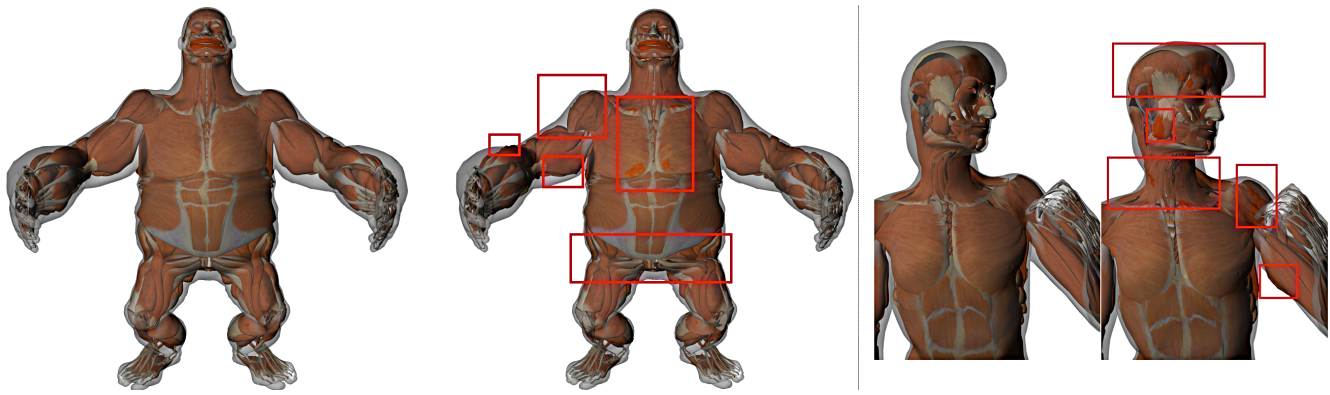


Figure 10: Left: our method. Right: the method of [Gilles et al. 2010] based on shape matching. Notice the artifacts of the latter method, e.g., the upper arm muscles intersecting the skin and asymmetry of the abdominal muscles.

413 morphograms (i.e. classes of shapes: big belly, big chest, or completely skinny) are available in the literature, but so far we found
414 no precise information on the corresponding fat distribution. More-
415 over, we do not model the fat tissue distributed anywhere else than
416 directly below the skin.
417

418 Other practical limitations are related to the registration. The skin
419 correspondence is inferred on a proximity basis. This sometimes
420 creates wrong results when the source and target characters are in
421 different poses. Our volumetric interpolation method does not guar-
422 antee foldover-free displacement field: although we did not observe
423 overlapping between internal structures in any of our examples, it
424 could occur in theory. The skin registration fails when the target
425 character has a different topology from the reference anatomy. For
426 the example shown in Fig. 5, we had to create a five-fingered variant
427 of the target character.

428 10 Conclusion

429 To address the high costs associated with anatomy authoring, we
430 have presented the first method for quickly creating a plausible
431 anatomy for any target character. For realistic humanoid models,
432 we transfer both the internal anatomical structures from a reference
433 model, as well as the fat thickness information extracted and retar-
434 geted from MRI data. Our method is thus purely automatic. For
435 cartoony characters, we offer a user friendly editing tool enabling
436 the user to tune the fat tissues of the target character. Transferring
437 the internal bones, viscera and muscles is then automatic.

438 We have shown that direct Laplace interpolation, perhaps sufficient
439 to generate simple effects such as muscle bulging, leads to objec-
440 tionable artifacts when used to transfer the full anatomy. Our spe-
441 cific pipeline ensures that basic anatomical rules are preserved.

442 In future work, we would like to take advantage of more anatomi-
443 cal knowledge to constrain the interpolations. We believe that our
444 method could also help the processing of body scans by computing
445 a first guess to the segmentation process, and complementing the
446 final result with thin structures, invisible in the volumetric image,
447 as shown by our validation example (Fig. 9).

448 Acknowledgements

449 Many thanks to Laura Paiardini and Armelle Bauer for 3D model-
450 ing and kind support. We would also like to thank the anonymous
451 reviewers for their detailed comments and feedback. This work was
452 partly funded by the French ANR SoHusim, the ERC Expressive

453 and CNRS Semyo projects.

454 References

- 455 AUBEL, A., AND THALMANN, D. 2001. Interactive modeling of
456 the human musculature. In *In Proceedings of Computer Anima-*
457 *tion*, 7–8.
- 458 BARAFF, D., AND WITKIN, A. 1998. Large steps in cloth sim-
459 ulation. In *Proceedings of the 25th annual conference on Com-*
460 *puter graphics and interactive techniques*, ACM, New York, NY,
461 USA, SIGGRAPH '98, 43–54.
- 462 BARAN, I., AND POPOVIĆ, J. 2007. Automatic rigging and ani-
463 mation of 3d characters. *ACM Trans. Graph.* 26, 3 (July).
- 464 BESL, P., AND MCKAY, N. 1992. A method for registration of 3-d
465 shapes. *IEEE Trans. PAMI* 14, 2, 239–256.
- 466 BINVOX, 2013. <http://www.cs.princeton.edu/~min/binvox/>.
- 467 BLEMKER, S., ASAKAWA, D., GOLD, G., AND DELP, S.
468 2007. Image-based musculoskeletal modeling: Applications, ad-
469 vances, and future opportunities. *Journal of Magnetic Resonance*
470 *Imaging* 25, 2, 441–451.
- 471 BRONSTEIN, A., BRONSTEIN, M., AND KIMMEL, R. 2008. *Nu-*
472 *merical Geometry of Non-Rigid Shapes*, 1 ed. Springer Publish-
473 ing Company, Incorporated.
- 474 FALOUTSOS, P., VAN DE PANNE, M., AND TERZOPOULOS, D.
475 2001. Composable controllers for physics-based character ani-
476 mation. In *Proceedings of the 28th annual conference on Com-*
477 *puter graphics and interactive techniques*, ACM, New York, NY,
478 USA, SIGGRAPH '01, 251–260.
- 479 GILLES, B., REVERET, L., AND PAI, D. 2010.
480 Creating and animating subject-specific anatomical
481 models. *Computer Graphics Forum* (June),
482 [http://onlinelibrary.wiley.com/doi/10.1111/j.1467-](http://onlinelibrary.wiley.com/doi/10.1111/j.1467-8659.2010.01718.x/abstract)
483 [8659.2010.01718.x/abstract](http://onlinelibrary.wiley.com/doi/10.1111/j.1467-8659.2010.01718.x/abstract).
- 484 GRAY, H., AND LEWIS, W. H. 1918. *Anatomy*
485 *of the human body*. Philadelphia: Lea and Febiger.,
486 <http://www.biodiversitylibrary.org/bibliography/20311>.
- 487 GUENNEBAUD, G., JACOB, B., ET AL., 2010. Eigen v3.
488 <http://eigen.tuxfamily.org>.
- 489 HUANG, Q.-X., ADAMS, B., WICKE, M., AND GUIBAS, L. J.
490 2008. Non-rigid registration under isometric deformations. In

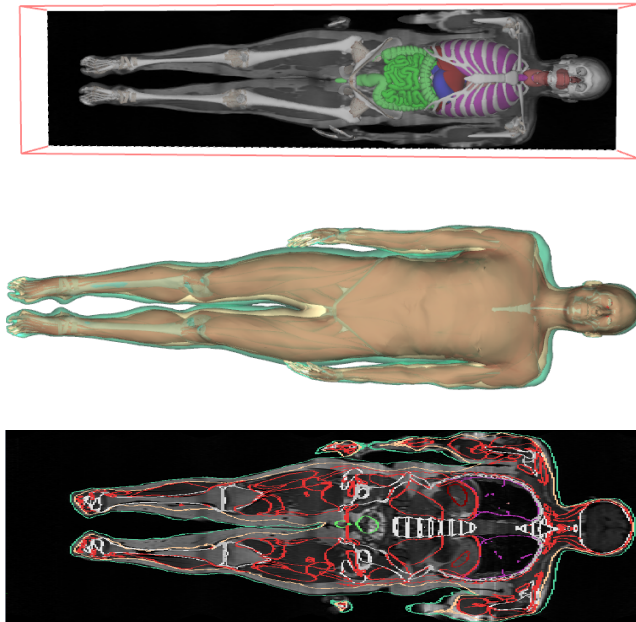


Figure 9: Transfer to an MRI image of a man laying on his back. Top: reconstruction of internal organs and skeleton within one slide of MRI Data. Center: reconstruction of muscular system. Bottom: comparison with the data. The green lines highlight our reconstructed surface, the beige lines correspond to the eroded volume, while the red line is muscle reconstruction, white and gray lines are bones and connectives tissues, the purple represents the lungs and the bright green represents the small intestine.

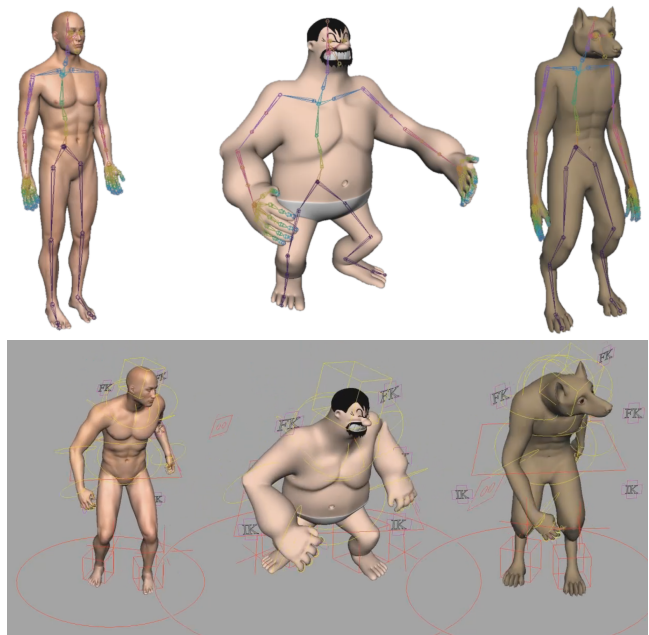


Figure 11: Top: Transfer of an articulated system. Bottom: Transfer of animation.

491 *Proceedings of the Symposium on Geometry Processing*, 1449–
492 1457.

493 JACOBSON, A., BARAN, I., POPOVIĆ, J., AND SORKINE, O. 2011. Bounded biharmonic weights for real-time deformation.
494 In *ACM SIGGRAPH 2011 papers*, ACM, New York, NY, USA,
495 SIGGRAPH '11, 78:1–78:8.

497 KAICK, O. V., ZHANG, H., HAMARNEH, G., AND COHEN-OR,
498 D. 2011. A survey on shape correspondence. *Computer Graph-
499 ics Forum* 30, 6, 1681–1707.

500 KAVAN, L., AND SORKINE, O. 2012. Elasticity-inspired deformer-
501 s for character articulation. *ACM Transactions on Graphics
502 (proceedings of ACM SIGGRAPH ASIA)* 31, 6, 196:1–196:8.

503 KAVAN, L., COLLINS, S., ZARA, J., AND O'SULLIVAN, C. 2008.
504 Geometric skinning with approximate dual quaternion blending.
505 *ACM Trans. Graph.* 27, 4, 105.

506 KRY, P. G., AND PAI, D. K. 2006. Interaction capture and synthe-
507 sis. *ACM Trans. Graph.* 25, 3, 872–880.

508 LEE, S.-H., AND TERZOPOULOS, D. 2006. Heads up!: biomechanical
509 modeling and neuromuscular control of the neck. In *ACM
510 SIGGRAPH 2006 Papers*, ACM, New York, NY, USA,
511 SIGGRAPH '06, 1188–1198.

512 LEE, S., SIFAKIS, E., AND TERZOPOULOS, D. 2009. Comprehen-
513 sive biomechanical modeling and simulation of the upper body.
514 *ACM Trans. Graph.* 28 (September), 99:1–99:17.

515 LI, H., SUMNER, R. W., AND PAULY, M. 2008. Global correspon-
516 dence optimization for non-rigid registration of depth scans. In

517 *Proceedings of the Symposium on Geometry Processing, SGP*
518 '08, 1421–1430.

519 LIPMAN, Y., AND FUNKHOUSER, T. 2009. Möbius voting for
520 surface correspondence. *ACM Trans. Graph., Proc. SIGGRAPH*
521 28, 3.

522 M. GILROY, BRIAN R. MACPHERSON, L. M. R. 2008. *Atlas of
523 anatomy*. Thieme.

524 MATEUS, D., HORAUD, R., KNOSSOW, D., CUZZOLIN, F., AND
525 BOYER, E. 2008. Articulated Shape Matching Using Laplacian
526 Eigenfunctions and Unsupervised Point Registration. In *IEEE
527 Conference on Computer Vision and Pattern Recognition (CVPR
528 '08)*, IEEE Computer Society, 1–8.

529 MAYA-MUSCLE, 2013. <http://images.autodesk.com/adsk/files/muscle.pdf>.

530 MOORE, K. L., AND DALLEY, A. F. 1999. *Anatomy Clinically
531 Oriented*, fourth ed. Lippincott Williams & Wilkins.

532 MÜLLER, M., HEIDELBERGER, B., TESCHNER, M., AND
533 GROSS, M. 2005. Meshless deformations based on shape
534 matching. *ACM Trans. Graph. (Proc. of SIGGRAPH)*, 471–478.

535 OVSIANIKOV, M., BEN-CHEN, M., SOLOMON, J., BUTSCHER,
536 A., AND GUIBAS, L. 2012. Functional maps: a flexible repre-
537 sentation of maps between shapes. *ACM Trans. Graph.* 31, 4,
538 30:1–30:11.

539 PATTERSON, T., MITCHELL, N., AND SIFAKIS, E. 2012. Simula-
540 tion of complex nonlinear elastic bodies using lattice deformer-
541 s. *ACM Trans. Graph.* 31, 6 (Nov.), 197:1–197:10.

542 POLLARD, N. S., AND ZORDAN, V. B. 2005. Physically based
543 grasping control from example. In *Proceedings of the 2005 ACM
544 SIGGRAPH/Eurographics symposium on Computer animation*,
545 ACM, New York, NY, USA, SCA '05, 311–318.

546 PRESS, TEUKOLSKI, VETTERLING, AND FLANNERY. 2002. *Nu-
547 merical Recipes in C++*. Cambridge University Press.

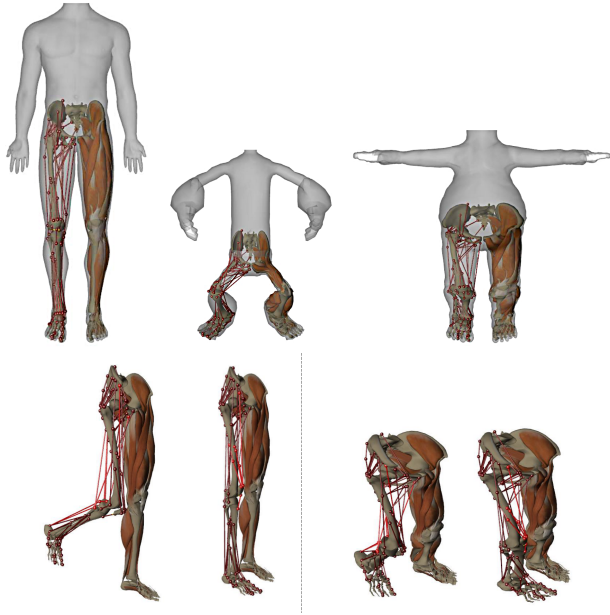


Figure 12: Top: Transfer of muscle lines of action. Bottom: knee movement using muscle control on both the source (zygote) and the target.

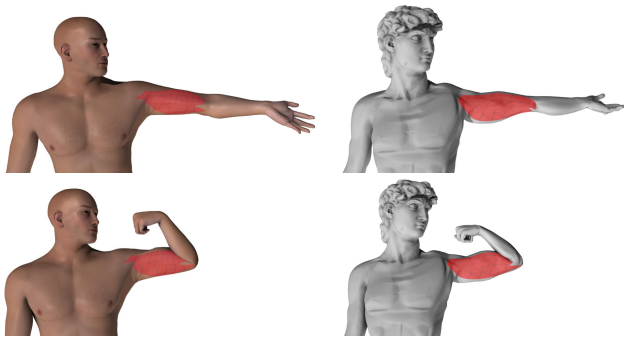


Figure 13: Top: Transfer of muscle and skin animation by using transferred muscles.

548 SCHEEPERS, F., PARENT, R. E., CARLSON, W. E., AND MAY,
 549 S. F. 1997. Anatomy-based modeling of the human musculature. In *Proceedings of the 24th annual conference on Computer graphics and interactive techniques*, ACM Press/Addison-Wesley Publishing Co., New York, NY, USA, SIGGRAPH '97, 163–172.
 550
 551
 552
 553
 554 SIFAKIS, E., NEVEROV, I., AND FEDKIW, R. 2005. Automatic
 555 determination of facial muscle activations from sparse motion
 556 capture marker data. *ACM Trans. Graph.* 24, 3.
 557
 558 SUEDA, S., KAUFMAN, A., AND PAI, D. 2008. Musculotendon
 559 simulation for hand animation. *ACM Transactions on Graphics* 27, 3, 83:1–83:8.
 560
 561 SUMNER, R. W., AND POPOVIĆ, J. 2004. Deformation transfer
 for triangle meshes. *ACM Trans. Graph.* 23, 3, 399–405.
 562
 563 THELEN, D. 2003. Adjustment of muscle mechanics model parameters to simulate dynamic contractions in older adults. *ASME*

125, 1, 70–77.
 565 WANG, J. M., HAMNER, S. R., DELP, S. L., AND KOLTUN,
 566 V. 2012. Optimizing locomotion controllers using biologically-
 567 based actuators and objectives. *ACM Trans. Graph.* 31, 4 (July),
 568 25:1–25:11.
 569 WATERS, K. 1987. A muscle model for animation three-
 570 dimensional facial expression. *SIGGRAPH Comput. Graph.* 21,
 571 4 (Aug.), 17–24.
 572 WEI, Q., SUEDA, S., AND PAI, D. K. 2010. Biomechanical simu-
 573 lation of human eye movement. In *Proceedings of the 5th inter-
 574 national conference on Biomedical Simulation*, Springer-Verlag,
 575 Berlin, Heidelberg, ISBMS'10, 108–118.
 576 WILHELMS, J., AND VAN GELDER, A. 1997. Anatomically
 577 based modeling. In *Proceedings of the 24th annual confer-
 578 ence on Computer graphics and interactive techniques*, ACM
 579 Press/Addison-Wesley Publishing Co., New York, NY, USA,
 580 SIGGRAPH '97, 173–180.
 581 ZHU, Y., SIFAKIS, E., TERAN, J., AND BRANDT, A. 2010. An
 582 efficient multigrid method for the simulation of high-resolution
 583 elastic solids. *ACM Transactions on Graphics (Presented at SIG-
 584 GRAPH 2010)* 29, 2, 16:1–16:18.
 585 ZORDAN, V. B., MAJKOWSKA, A., CHIU, B., AND FAST, M.
 586 2005. Dynamic response for motion capture animation. *ACM
 587 Trans. Graph.* 24, 3 (July), 697–701.